Quaternary Science Reviews 29 (2010) 1817–1830

Contents lists available at ScienceDirect

Quaternary Science Reviews

journal homepage: www.elsevier.com/locate/quascirev

Quaternary glaciation of Gurla Mandhata (Naimon'anyi)

Lewis A. Owen [a,*], Chaolu Yi [b], Robert C. Finkel [c], Nicole K. Davis [a]

[a] Department of Geology, University of Cincinnati, Cincinnati, OH 45221, USA
[b] Institute for Tibetan Plateau Research, Chinese Academy of Sciences, Beijing, 100085, China
[c] Department of Earth and Planetary Sciences, University of California, Berkeley, CA 95064 USA and Centre Européen de Recherche et d'Enseignement des Géosciences de l'Environnement, 13545 Aix en Provence Cedex 4, France

ARTICLE INFO

Article history:
Received 21 December 2009
Received in revised form
25 March 2010
Accepted 30 March 2010

ABSTRACT

The Quaternary glaciation of Gurla Mandhata (Naimona'nyi), an impressive, isolated dome-shaped massif situated in a remote region of southern Tibet, was examined using glacial geomorphic methods and dated using ^{10}Be terrestrial cosmogenic nuclides. The oldest moraines, representing an expanded ice cap that stretched ~ 5 km into the foreland of the Gurla Mandhata massif, likely formed during marine isotope stage (MIS) 10 or an earlier glacial cycle. Another glacial expansion of coalescing piedmont type occurred during the early part of the last glacial cycle or the penultimate glacial cycle, after which glaciers became restricted to entrenched valley types. Impressive latero-frontal moraines at the mouths of most valleys date to the early part of the last glacial cycle and MIS 3. A succession of six sets of moraines within the valleys and up to the contemporary glaciers show that glaciers advanced during the Lateglacial, Early Holocene, Neoglacial and possibly Little Ice Age. The change of style of glaciation throughout the latter part of the Quaternary, from expanded ice caps to deeply entrenched valley glaciers, might reflect: (1) climatic controls with reduced moisture supply to the region over time; and/or (2) tectonic controls reflecting increase basin subsidence due to detachment faulting and enhanced valley incision.

1. Introduction

Gurla Mandhata (Naimona'nyi) is an impressive isolated dome-shaped massif situated in a remote region of southern Tibet (Figs. 1 and 2). The massif lies just north of the Greater Himalaya among the source waters of four major Himalayan river systems: the Indus, Sutlej, Ganges and Tsangpo-Brahmaputra. The glacial geologic record of Gurla Mandhata has the potential to provide important information on the nature of glaciation at the headwaters of these immense river systems, which in turn has important implications for understanding past and predicting future hydrological changes in a transforming climate. Furthermore, Gurla Mandhata is one of the best examples of an evolving massif linked to a crustal-scale detachment system along the Himalayan–Tibetan orogen (Murphy et al., 2002) and provides an excellent natural laboratory to examine the relationships among tectonics, climate, glaciation, erosion and landscape development. To develop a framework for glacial geologic, geomorphic, and paleoclimate studies in this region, we examine the glacial geologic record of the massif and determine the extent and timing of past glaciation using remote sensing, field mapping, the examination of glacial and associated landforms, and we date glacial landforms using ^{10}Be terrestrial cosmogenic nuclide (TCN) surface exposure dating methods.

2. Study area

Gurla Mandhata (30.4°N/81.2°E) is located in the Nalakankar Himal in southern Tibet near the southeastern terminus of the >1000-km long right-slip Karakoram fault, between the Main Central Thrust and the Southern Tibetan detachment system to the south and the South Kailas Thrust and the Indus-Yalu Suture Zone to the north. The massif rises from ~3800 m above sea level (asl) to the 34th highest mountain in the world, Gurla Mandhata, at 7694 m asl over a distance of ~25 km, and is drained by the Karnali River, which flows south along the west side of the massif and turns abruptly east before crossing the divide of the Greater Himalaya into Nepal where it flows into the Seti River. Two large lakes, La'nga Co (4572 m asl; also called Raksas) and Mapam Yum Co (4586 m asl; also called Manasarovar) are located ~5 km north of the mountain. Today there are cirques, valley glaciers, and a small ice cap on the massif.

Gurla Mandata is bounded to the west by a normal fault system – the Gurla Mandhata detachment system – which has exhumed

* Corresponding author. Fax: +1 513 556 4203.
E-mail address: lewis.owen@uc.edu (L.A. Owen).

0277-3791/$ – see front matter © 2010 Elsevier Ltd. All rights reserved.
doi:10.1016/j.quascirev.2010.03.017

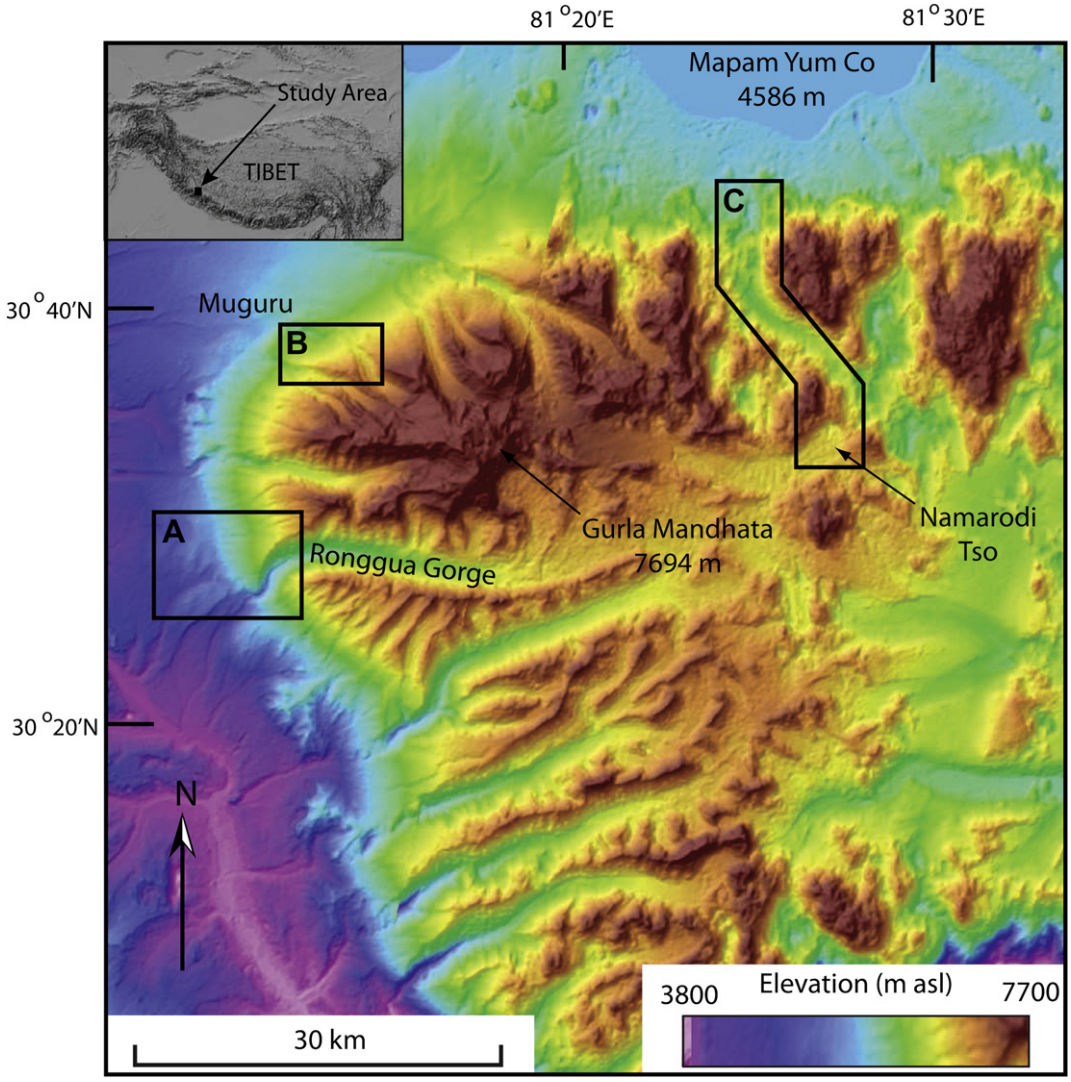

Fig. 1. Digital elevation model (produced from ASTER data) of Gurla Mandhata showing the locations of the detailed study areas. (A) Ronggua valley foreland; (B) Muguru valley; (C) Namarodi valley. Inset shows regional location of the study area.

mid-crustal rocks of the Greater Himalayan Crystalline Sequence (Murphy et al., 2002) which core the massif. Using field mapping and geochronologic and thermobarometric analyses, Murphy et al. (2002) showed that Gurla Mandhata underwent major middle to late Miocene east-west extension along the Gurla Mandhata detachment system. The maximum fault slip occurred along a pair of low-angle normal faults that have caused significant tectonic denudation of the Tethyan Sedimentary Sequence, resulting in juxtaposition of weakly metamorphosed Paleozoic rocks and Tertiary sedimentary rocks in the hanging wall over amphibolite-facies mylonitic schist, marble, gneiss, and variably deformed bodies of leucogranite in the footwall. Murphy et al. (2002) argue for a total slip of between 66 and 35 km across the Gurla Mandhata detachment system, comparable to estimates of slip on the right-slip Karakoram fault system, to which it is interpreted to be kinematically linked. Together with the Karakoram Fault, the Gurla Mandhata detachment system produced the Pulan Basin, which became filled with Neogene sediments (Murphy et al., 2002). Cooling ages on minerals within the massif and geochronologic data on the movement of the Karakoram Fault indicate that the Gurla Mandhata massif has been forming over the last 10–20 Ma, and that the majority of the uplift had occurred by ~8 Ma as a result of extension (Murphy et al., 2000, 2002). Normal faulting continues today, as is evident from fresh fault scarps along the western margin of the massif, widening the pull-apart basin west of the massif.

Ma (1989) showed that the glacial geomorphology of the massif records changes in glacial style over time from expanded ice cap, to piedmont, and to entrenched valley glaciation, culminating in a phase of rock glacierization, but he did not speculate on the cause for these changes in glacial style (Fig. 3; Table 1). Through correlation with other parts of the Himalaya and Tibet, Ma (1989) suggested ages for the four major glaciations he recognized (Table 1). Contemporary glaciers are inset into deep, box-shaped valleys (Fig. 2) and are largest on the eastern slopes of the massif. In total there are 58 glaciers in the region covering a total area of ~80 km^2, but none of these glaciers extend below 5320 m asl (Ma, 1989). These are cirque or valley glaciers of cold-based continental type (Benn and Owen, 2002).

The region has a cold arid continental climate. The only major town in the region, Burang (~20 km SW of the summit of Gurla Mandhata and at ~3900 m asl), has a mean annual temperature of 3 °C and a mean annual precipitation total of 176 mm from 1973 to 1984 (Miehe et al., 2004). The mean monthly precipitation record displays two peaks of approximately equal magnitude (~25 mm) in March–April and August–September. The precipitation that occurs

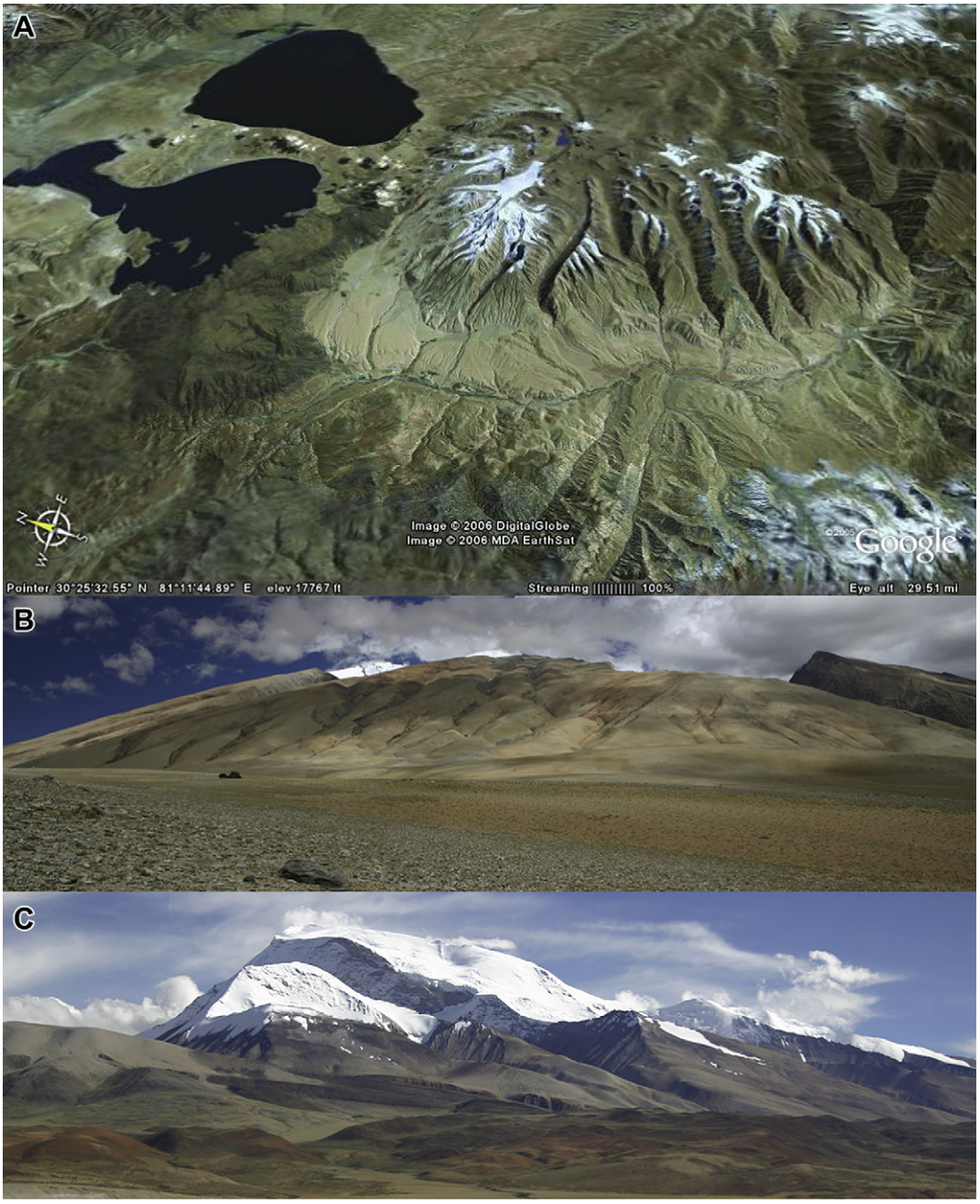

Fig. 2. Views of Gurla Mandhata. (A) Google Earth image viewed E/NE showing foreland, and La'nga Co (Co = lake) and Mapam Yum Co. (B) View of the western slopes showing glaciated foreland; and (C) view E/SE across Gurla Mandhata illustrating deeply entrenched glacial valleys.

in late winter is likely transported to the area by the westerly winds, while the late summer precipitation is most likely carried inland by the monsoon. In contrast, precipitation is significantly higher to the south and east, and to the west of Gurla Mandhata because of the influence of the monsoon and the mid-latitude westerlies, respectively.

3. Methods

3.1. Field methods

The geomorphology of the region was studied in the field, aided by interpretation of Google Earth and ASTER imagery. Detailed studies were undertaken in three areas: (i) the Ronggua valley foreland; (ii) the Muguru valley; and (iii) the Namarodi valley (Fig. 1). These regions were chosen based on their logistical and political accessibility, and to provide some areal coverage of the massif. The chronology of Ma (1989) was examined and evaluated. Moraines of the Naimona'nyi (oldest) and Rigongpu glaciations were very distinctive and we call these M1 and M2, respectively. Individual moraines within the Naimona'nyi glacial moraines were further subdivided into M1a, M1b and M1c to differentiate distinct moraine ridges for sampling. Moraines of Ma's (1989) Namorangre glaciation were subdivided into M3 and M4 based on relative position and morphostratigraphy. M4 moraines were further subdivided into M4a, M4b and M4c to differentiate distinct moraine

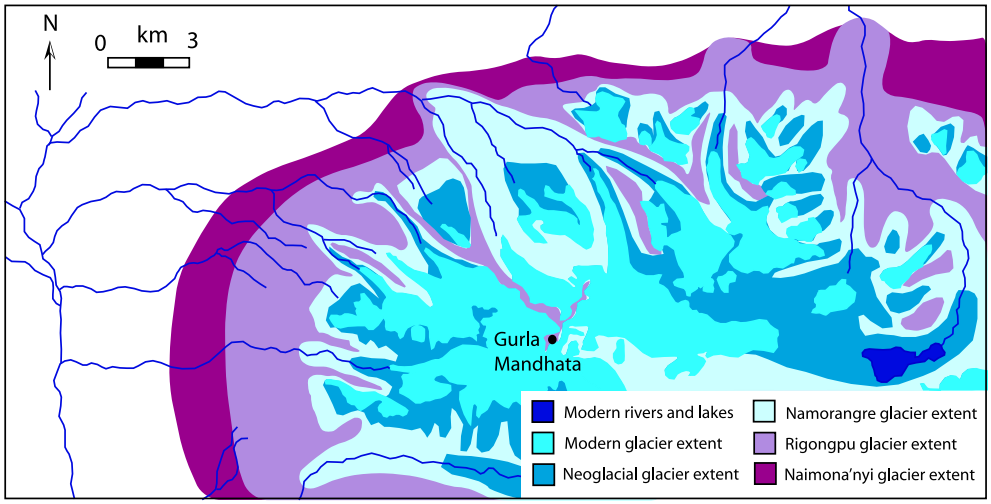

Fig. 3. Reconstructions of the former extents of glaciation on Gurla Mandhata (after Ma, 1989).

ridges for sampling. The Neoglacial moraines of Ma (1989) comprise at least six sets of moraines and we subdivide these sequentially from M5 to M10 (youngest). Moraines with the same number in different regions correlate with each other. Glacial and associated landforms were mapped in the field and sedimentary deposits were examined using the methods summarized in Benn and Owen (2002).

3.2. Sampling for ^{10}Be TCN dating

Samples for ^{10}Be TCN surface exposure dating were collected from moraines in each of the three study areas and from bedrock in the Namarodi valley (Figs. 4–9). The geomorphic characteristics of the boulders, moraines, and the sample sites, including boulder size, degree of weathering, whether surfaces had glacial polish/striations, and the degree of burial within sediment, were noted to assess whether there might have been any post-depositional modification of the exposed surfaces. The lithology and thickness of the sample, and if applicable, the dip of the sample surface were also recorded. The angle from the sampling sites to the horizon was recorded to make corrections for topographic shielding.

Table 1
Geomorphic description and inferred ages for Ma's (1989) four major glaciations of the Gurla Mandhata massif.

Glacial stage	Geomorphic character	Proposed age
Naimona'nyi	Morainic platform in the foreland of the massif extending to ~4400 m asl. This is characterized by scattered erratics and gravel–rich surfaces with soil developed to a depth of >20 cm	Middle Pleistocene based on correlation with moraine platforms on the north slope of the West Kunlun that had a thermoluminescence age of 333 ± 46 ka.
Rigongpu	Less extensive till sheet with scattered erratics in the foreland of the massif that extend from 4600 m asl and fan-shaped moraines (of piedmont glacier type) at ~4800 m asl.	Early Late Pleistocene based on radiocarbon dating of calcium carbonate taken from piedmont moraines (presumably cements) that had radiocarbon ages of 40.1 ± 1 ka, 33.25 ± 0.75 ka and 32.9 ± 0.8 ka.
Namorangre	End moraines, containing large boulders, some of which extend into foreland and others are confined to valleys/cirques.	Late Pleistocene, no explanation given, but likely based on correlation with moraines elsewhere in Tibet.
Neoglacial	Three sets of small end moraines, mostly confined to valleys and cirques	Holocene, no explanation given, but likely based on correlation with moraines elsewhere in Tibet.

3.3. Laboratory methods for TCN dating

Rock samples were crushed and sieved to obtain the 250–500 μm size fraction. This fraction was chemically leached using a minimum of four acid leaches: aqua regia for >9 h; two 5% HF/HNO_3 leaches for ~24 h; and one or more 1% HF/HNO_3 leaches each for ~24 h. A heavy liquid (lithium heteropolytungstate) separation was used after the first 5% HF/HNO_3 leach. The pure quartz that was obtained was spiked with a Be carrier that had a $^{10}Be/^{9}Be$ ratio of $2.99 \pm 0.22 \times 10^{-15}$. The spiked quartz was dissolved in concentrated HF and then fumed three times with perchloric acid. Samples were then passed through anion and cation exchange columns to separate the Be fraction. Ammonium hydroxide was added to the Be fractions to precipitate beryllium hydroxide gel. $Be(OH)_2$ was oxidized by ignition at 750 °C for 5 min in quartz crucibles. The resultant BeO was mixed with Nb powder and loaded in steel targets for the measurement of the $^{10}Be/^{9}Be$ ratios by accelerator mass spectrometry at the Center for Accelerator Mass Spectrometry at Lawrence Livermore National Laboratory. All ^{10}Be TCN ages for boulder samples were calculated by applying the Lal (1991) and Stone (2000) time-independent model using the CRONUS Earth 2.2 calculator (Balco et al., 2008b; http://hess.ess.washington.edu/math/), with a production rate of 4.5 ± 0.3 ^{10}Be atoms/gram of quartz/year and isotope ratios were normalized to ^{10}Be standards prepared by Nishiizumi et al. (2007) with a value of 2.85×10^{-12}, and using a ^{10}Be half life of 1.36×10^{6} years and rock density of 2.7 g/cm^3.

The two oldest samples, NA1 and NA7, were used to calculate erosion rates using the methods of Lal (1991) to provide a weighted mean erosion rate of 1.2 m/Ma. Erosion rates of 1.2 m/Ma would cause an age of 1 ka to be underestimated by <0.5%, 10 ka age by ~1%, 20 ka age by ~2%, 40 ka age by ~4%, 100 ka by ~10%, 200 ka by ~21% and 400 ka by ~58%.

4. Study area descriptions

4.1. Ronggua Gorge foreland

The Ronggua Gorge foreland study area is situated along the western slopes of Gurla Mandhata and transverse the main normal

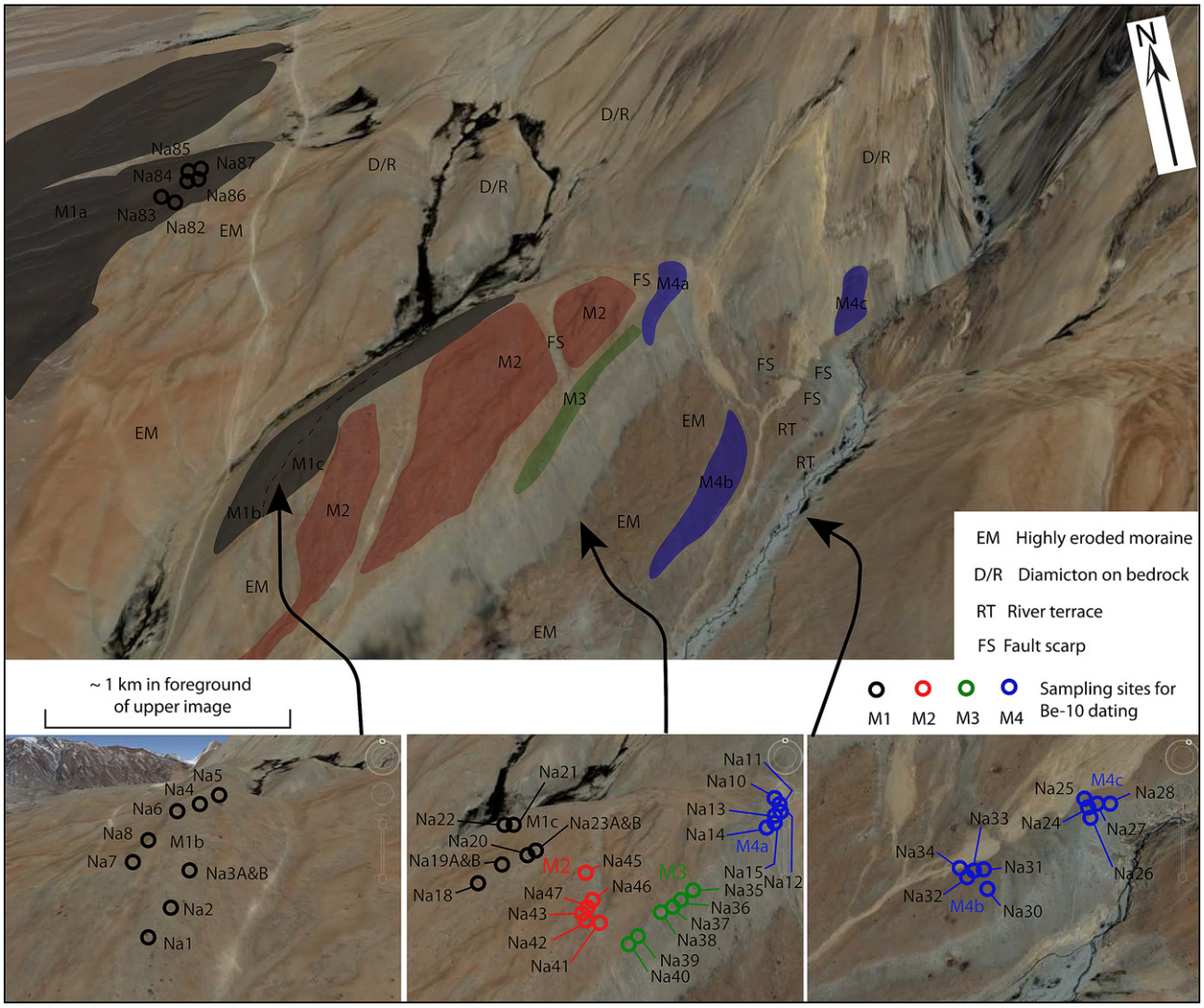

Fig. 4. Google Earth images showing the glacial landforms and sampling locations for ^{10}Be TCN dating for the Ronggua valley foreland.

fault system of the Gurla Mandhata detachment system (Figs. 1 and 4). The westernmost extent of the study area borders impressive terraces that Murphy et al. (2002) interpreted as eroded Neogene valley fill deposits. The main study area is traversed by an impressive stream that forms a deep canyon within the main Gurla Mandhata massif. The oldest glacial deposits comprise the "morainic platform" of the Naimona'nyi glaciation (Ma, 1989) and form a till sheet with large (2 m diameter) glacial boulders scattered across the landscape. This till sheet is characterized in part by very subdued ridges that broadly follow the outline of the present mountain front. We call these the M1 moraines and we collected samples for ^{10}Be dating from large boulders at three separate locations (M1a, M1b and M1c; Figs. 4 and 5A–C). Glacial boulders from the M1 moraines are well inset into the substrate and are well weathered, with cm-deep cavernous weathering voids, and some boulders have rims weathered flat to the surface (Fig. 5C), while other boulders are completely weathered flush to the surface.

Nearer to the mountain front, subdued ridges are present radiating from the mountain front valley exit. Ma (1989) interpreted these as moraines formed by piedmont glaciers that advanced into the foreland during the Rigongpu glaciation. These moraine ridges have scattered glacial boulders inset into the surface and the boulders are deeply weathered. We call these moraines M2 and sampled boulders on one of the ridges for ^{10}Be dating (Figs. 4 and 5D).

Two sets of moraines are present near the stream that exits the mountain front. Ma (1989) assigns these moraines to the Namorangre glaciation (our M3 and M4). The older and more extensive moraine (M3) forms a prominent ridge rising several tens of meters above and along the contemporary valley (Figs. 4 and 5E). Meter-size boulders are abundant on this moraine. The boulders are weathered, but few exhibit cavernous weathering. Boulders on the dominant ridge were sampled for ^{10}Be dating (Figs. 4 and 5E).

A series of small end moraines are present at the mouth of the main stream at the mountain front. These moraines rise ~10–20 m above the stream and are displaced by normal faults (M4a, M4b and M4c). Boulders present on these moraines exhibit slight granular weathering. Boulders on all three moraines were sampled for ^{10}Be dating (Figs. 4 and 5F–H).

4.2. Muguru valley

The Muguru valley faces NW and contains two valley glaciers that extend to ~5500 m asl (Fig. 6). The valley contains at least seven sets of latero-frontal moraines, which we number M4 through M10. The oldest moraine (M4) forms an arc-shaped ridge at the mouth of the valley, which rises about 15–20 m above the

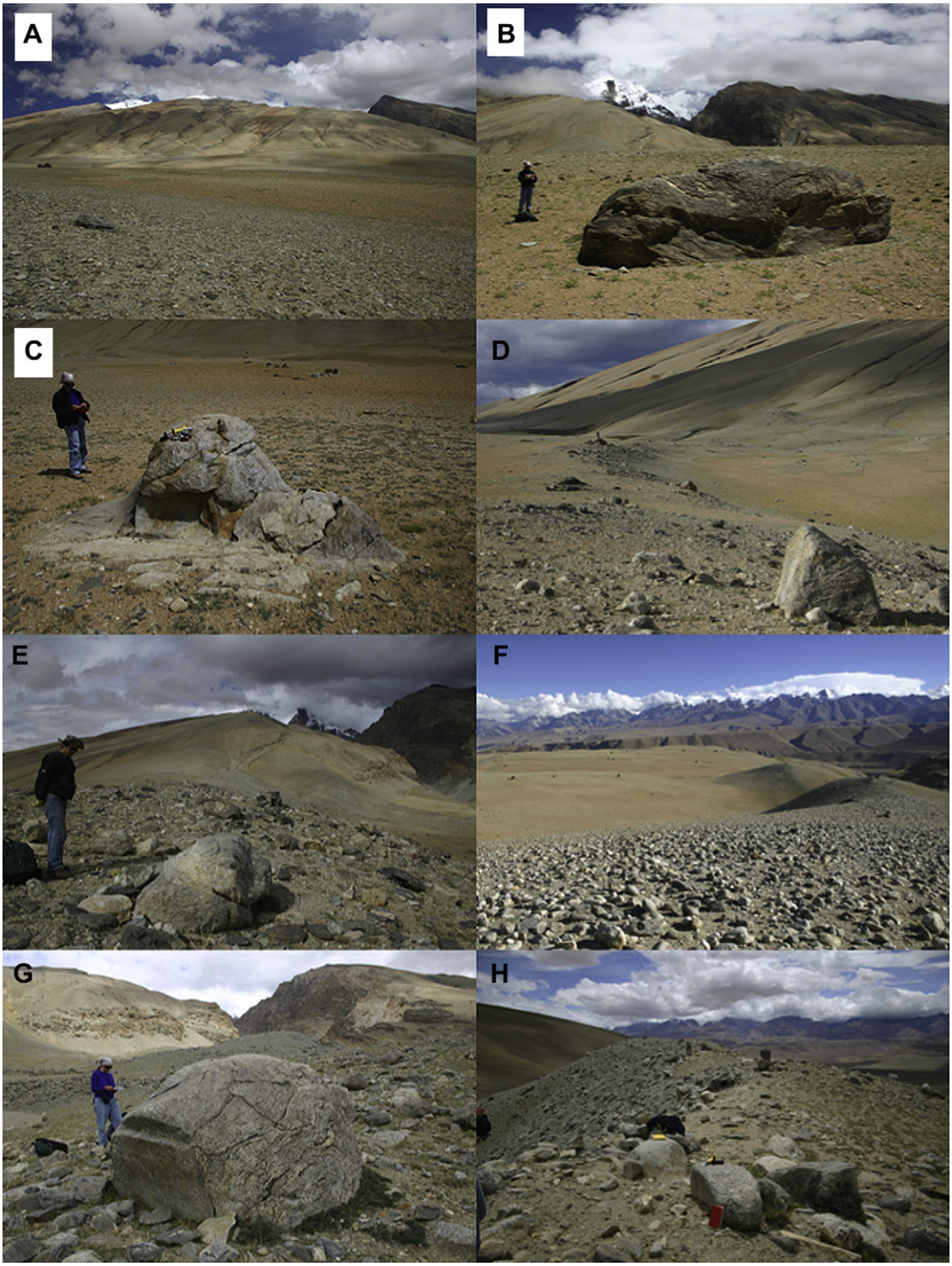

Fig. 5. Glacial landforms in the Ronggua valley foreland. (A) Views looking E across the M1A moraine towards Gurla Mandhata. (B) View of typical sampled boulder (sample NA7) on the M1B moraine. (C) Intensely weathered boulder (sample NA23) on M1C. (D) View NE looking up the M2 moraine. (E) View E along M3 moraine. (F) View SW along the M4A moraine. (G) View of typical sampled boulder (sample NA31) on the M4B moraine. (H) View along M4C moraine showing the location of boulder sample NA9.

main valley floor (Figs. 6 and 7A). The moraine has large boulders on its crest that exhibit slight granular disintegration, which were sampled for ^{10}Be dating (Fig. 7A). Ma (1989) assigned this moraine to the Namorangre glaciation. The next moraine up valley (M5) is very subdued and has few boulders on its surface and was not sampled for ^{10}Be dating.

Farther up valley are three sets of latero-frontal moraines that rise between 10–20 m above the valley floor. These are the Neoglacial moraines of Ma (1989) and we number them M6, M7 and M8 (Fig. 6). The surfaces of these moraines contain scattered boulders that exhibit very slight granular weathering (Fig. 8B–D). Boulders on all three were sampled for ^{10}Be dating.

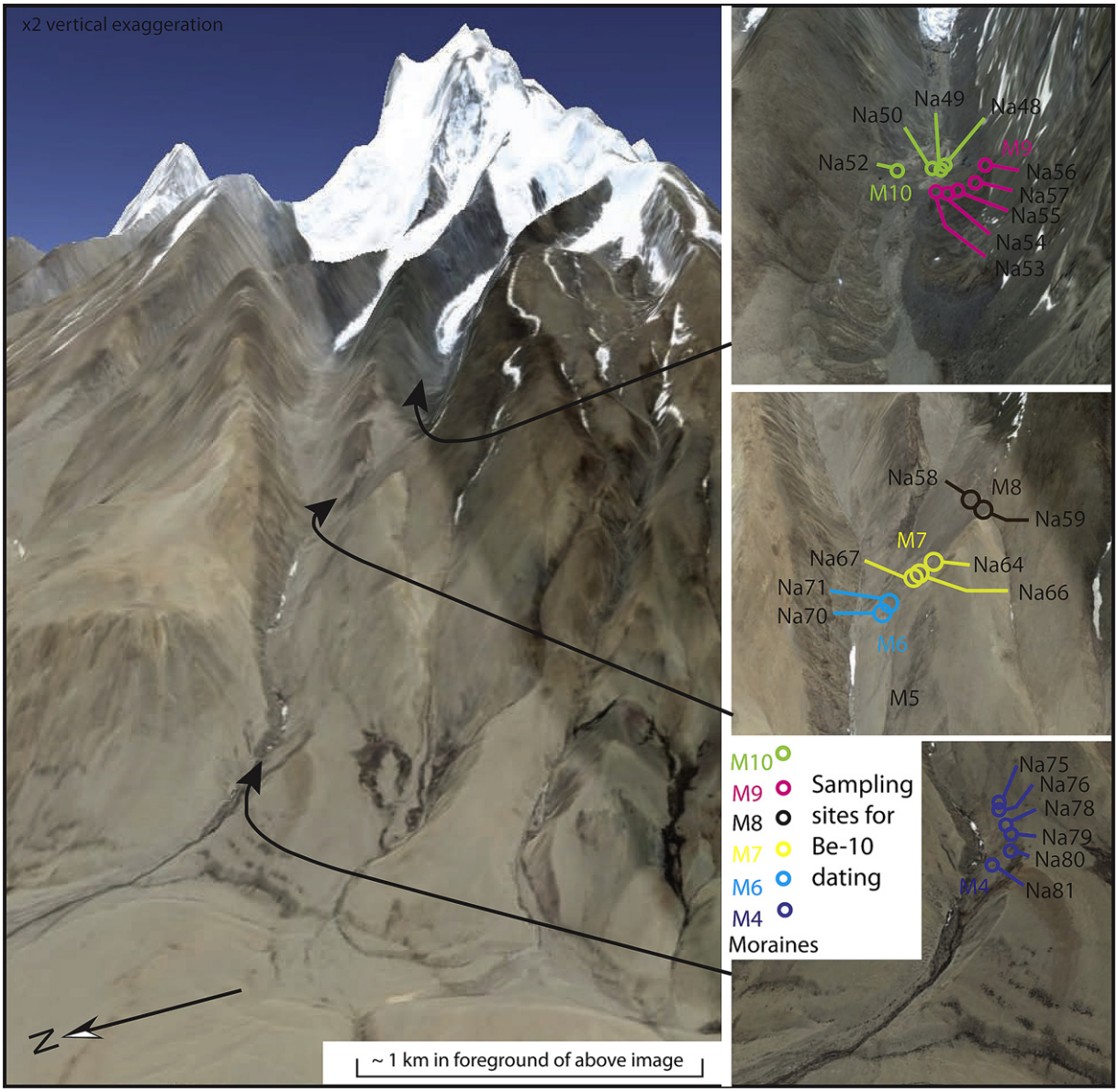

Fig. 6. Google Earth images showing the glacial landforms and sampling locations for ^{10}Be TCN dating along the Muguru valley.

Two sets of moraines are present within a few hundred meters of the contemporary glaciers, comprising sharp crested latero-frontal moraines with abundant unweathered, meter-sized boulders on their surfaces (Figs. 6, and 7E and F). These moraines were numbered M9 and M10, and boulders for ^{10}Be dating were collected from both. Impressive rock glaciers are present down valley between M8 and M10.

4.3. Namarodi valley

The Namarodi valley study area stretches from the east side of Namarodi Tso (Tso means Lake) to the foreland of the Gurla Mandhata massif south of Mapam Yum Co (Fig. 8). Two sets of impressive moraines (M4a and M4b) are present at the mouth of the Namarodi valley at ~4800 m asl representing piedmont glaciers of the Namorangre glaciation of Ma (1989). These moraines rise several tens of meters above the foreland and are comprised of multiple ridges. Abundant meter-size boulders are present on these moraines, which exhibit slight granular weathering. Boulders on both sets of moraines were sampled for ^{10}Be dating (Figs. 8, 9A and B).

Small rock glaciers and rock glacierized slopes are abundant between the mouth of the Namarodi valley to ~5500 m asl. Glacially polished bedrock surfaces and a subdued moraine are present at ~5000 m asl, just to the east of Namarodi Tso (Figs. 8 and 9C), which we call M5 and Ma (1989) assigned to the Neoglacial. Samples for ^{10}Be dating were collected from boulders on this moraine and from the glacially eroded bedrock surfaces (Figs. 8 and 9C).

An impressive end moraine (M6) is present on the west side of Namarodi Tso several hundred meters from the contemporary glacier, rising ~30 m above the lake, (Figs. 8, 9E and F). Abundant meter-size boulders, some of which exhibit granular weathering, are present on the moraine. These were sampled for ^{10}Be dating.

5. Dating results

The ^{10}Be dating results are shown in Table 2. Problems associated with the application of surface exposure dating

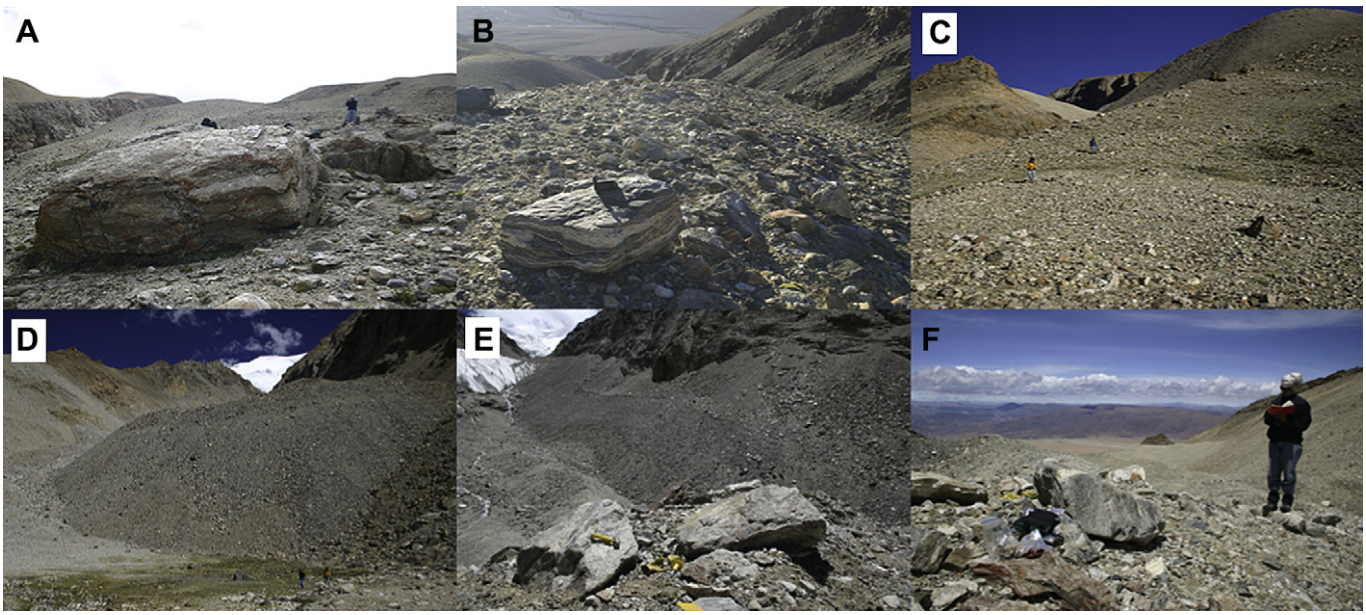

Fig. 7. Glacial landforms in the Muguru valley. (A) View of typical sampled boulder (NA76) on the M4 moraines. (B) View looking west along the M6 moraine showing sampled boulder NA70. (C) View E up the M7 moraine. (D) View E at the latero-frontal moraine of the M8 moraine. (E) View of sampled boulder NA55 on the M9 moraine with the M10 moraine in the distance. (F) View of sampled boulder (NA9) on the M10 moraine.

methods to date moraines in the Himalaya and Tibet, and elsewhere, has been discussed in detail in previous work (e.g. Hallet and Putkonen, 1994; Benn and Owen, 2002; Owen et al., 2002, 2003a, 2005, 2006a, 2008, 2009; Putkonen and Swanson, 2003; Putkonen and O'Neal, 2006; Seong et al., 2007, 2008, 2009; Putkonen et al., 2008). These problems include uncertainty introduced in the calculation of the production rate of TCNs and geologic complexities affecting surfaces such as

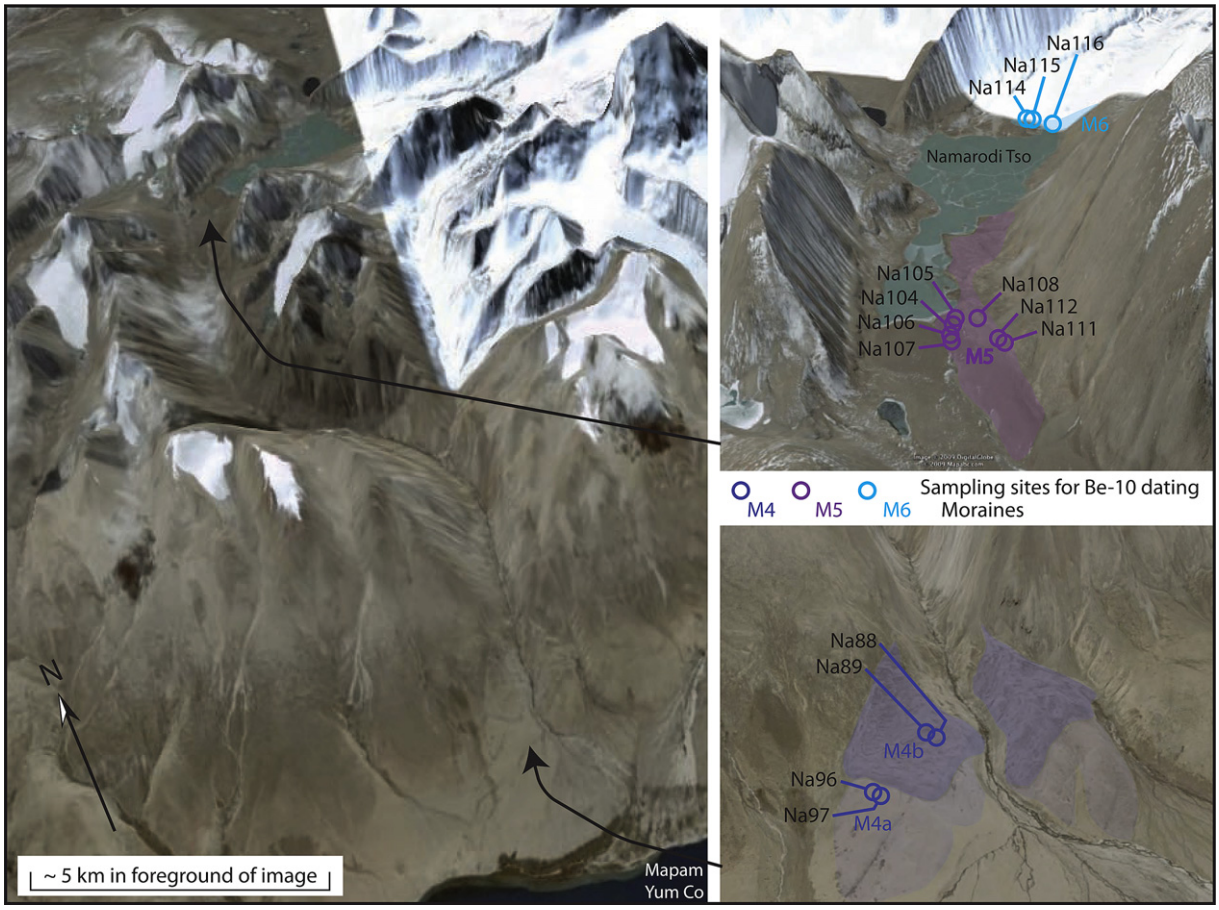

Fig. 8. Google Earth images of glacial landforms and sampling locations for ^{10}Be TCN dating along the Namarodi valley.

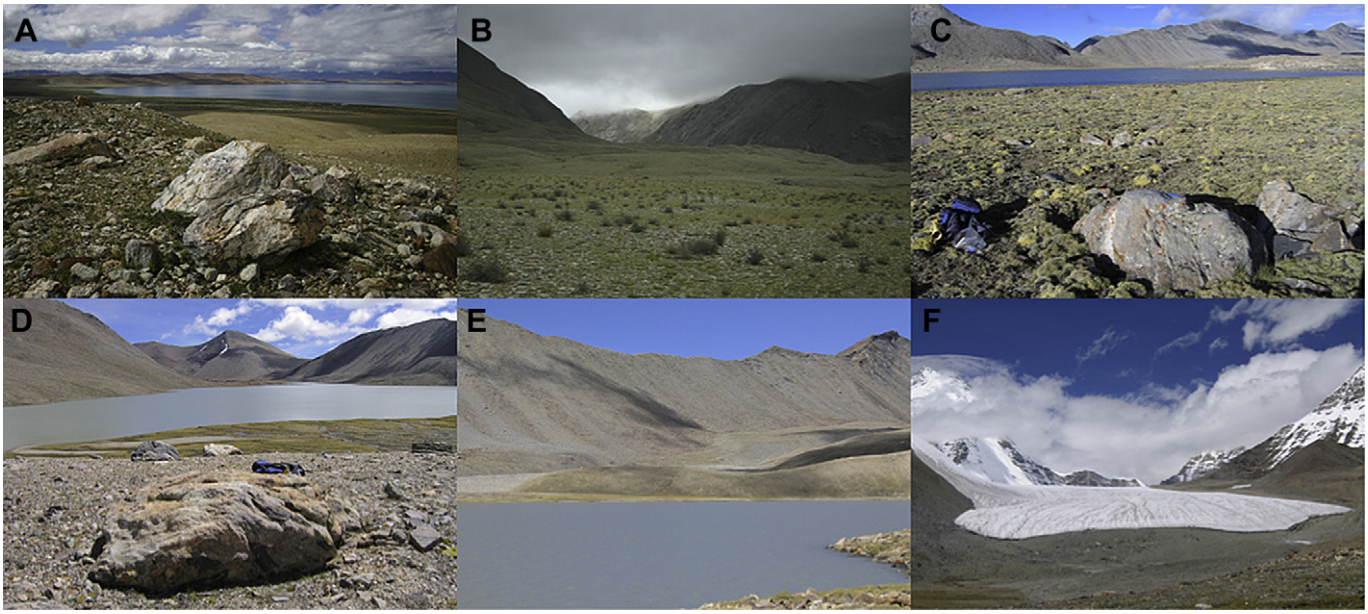

Fig. 9. Glacial landforms in the Namarodi valley. (A) View NW across M4A moraine showing a boulder that was sampled (NA96). (B) M4B moraine viewed looking south into the Namarodi valley. (C) View SW across the M5 moraine with Namarodi Tso in the distance. The boulder in the foreground was sampled for ^{10}Be dating (sample NA106). (D) M6 moraine viewed eastward looking down valley, showing sampled boulder NA115. (E) View looking S/SW at M6 at the western end of Namarodi Tso. (F) View of the M6 moraine showing young moraines, possibly historical, around the contemporary glacier.

weathering, exhumation, prior exposure and shielding of the surface by snow and/or sediment. Balco et al. (2008a, b) and Owen et al. (2008) highlighted the large uncertainty associated with different scaling models for low-latitude and high-altitude locations such as the Himalaya and showed that there may be as much as 40% difference between scaling models over the last glacial. Much of this difference is due to the uncertainty in correcting for variations in the geomagnetic field intensity, and currently there is much debate regarding the appropriate scaling model that should be used. Given these problems, we apply the Lal (1991) and Stone (2000) time-independent models, but recognize the uncertainty in our calculated ages and use caution when assigning our numerically dated moraines to particular climatostratigraphic times.

The geologic factors that complicate dating moraines often overshadow those associated with production rates, especially when the moraines are of great antiquity (many 100s of thousands of years old). These factors generally reduce the concentration of TCNs in rock surfaces, which results in an underestimate of the true age of the landforms and can result in a large spread in apparent exposure ages on a landform. Episodes of prior exposure of rock surfaces are an exception and result in an overestimate of the true age of the moraine. Putkonen and Swanson (2003) argued, however, that only a few percent of dated moraine boulders have had prior exposure. These effects can be partially assessed by collecting multiple samples on a surface that is being dated and assigning an appropriate age based on the distribution of TCN ages. However this is another area of debate and contention, since some researchers argue that the oldest age in a cluster of ages on a moraine (e.g. Briner et al., 2005) is the most appropriate measure of the true age of the landform, while others suggest that statistically analyzing the clustering of the ages, such as applying the mean square of weighted deviates method (e.g. Dortch et al., 2010), is more appropriate. In an attempt to be objective, we plot all our ages for each moraine as stacked probability distribution plots and show the range of ages in Fig. 10 and list the maximum age, average and range of ages per moraine in Table 3. We assign our best estimate of the age of the moraine given the distribution of ages on each moraine and by examining the morphostratigraphic context of each moraine in relation to its adjacent moraines (Table 3).

The oldest moraines, of Ma's (1989) Naimona'nyi glaciation and our M1a–c moraines, were sampled in the foreland of the Ronggua Gorge, and included three distinct moraines. These had exposure ages that ranged from 78–482 ka, but have an average of 281 ± 116 ka (error $= 1\sigma$). M1b and M1c have 4 and 5 boulders older than 300 ka, respectively, while M1 has one older than 300 ka. Given the deep weathering of most of the boulders on these moraines and the large number of boulders older than 300 ka, we argue that these moraines are very much older than 300 ka, but cannot assign a precise age to their formation, suffice to say that they might have formed during marine isotope stage (MIS) 10 or earlier.

^{10}Be ages for boulders on Ma's (1989) Rigongpu moraines, our M2 moraines, range from 62 to 107 ka, with an average of 79 ± 17 ka. We suggest that these formed in the early part of the last glacial cycle, or the penultimate glacial cycle if we consider the younger ages to be the result of weathering and/or erosion and older ^{10}Be ages to be more representative of the true of the landform.

Boulder ages for M3, Ma's (1989) Namorangre glaciation, at the mouth of the Ronggua Gorge range from 28 to 64 ka and show that it formed during the early part of the last glacial cycle. However, the large spread of ages does not allow us to distinguish whether it formed during MIS 4 or MIS 3.

The ^{10}Be ages for boulders on latero-frontal moraines, M4a–c, at the mouth of the Ronggua Gorge all cluster reasonably well with a mean age of 40 ± 9 ka. M4a at the mouth of the Namarodi valley provides a similar age at 52 ± 2 ka. In contrast, M4b has young ages, ~15 ka, and given their context and the degree of erosion it is likely these ages reflect exhumation or toppling of boulders. Given that weathering rates of ~1 m/Ma would only affect the age by a few percent, we argue that the M4 moraines formed during MIS 3.

^{10}Be ages (~15–0.1 ka) for boulders on Ma's (1989) Neoglacial moraines, our M5–10 moraines, show that the moraines span a longer duration than the Neoglaciation. Exposure ages from M5 and M6 in the Namarodi valley (12.4–15.3 ka) span the Lateglacial, but the clustering of boulders was not sufficient to assign them to

Table 2
Sample locations, descriptions, chemistry and ^{10}Be ages.

Sample number	Landform	Latitude (°N)	Longitude (°E)	Altitude (m asl)	Boulder size a/b/c axis (cm)	Sample thickness (cm)	Shielding correction	^{10}Be atoms 10^4 per g of SiO_2	Age[a] (ka)	External error[b] (ka)
Ronggua Gorge Foreland										
Na24	M4c	30.3791	81.1844	4433	190/170/90	1	1	254.2 ± 5.97	37.7 ± 0.9	3.4
Na25	M4c	30.3792	81.1843	4432	100/100/80	0.5	1	280.05 ± 5.45	41.5 ± 0.8	3.7
Na26	M4c	30.3789	81.1844	4433	170/100/70	3	1	304.7 ± 10.24	46.1 ± 1.6	4.3
Na27	M4c	30.3792	81.1845	4438	130/100/45	1.5	1	148.12 ± 2.71	21.9 ± 0.4	2.0
Na28	M4c	30.3794	81.1847	4438	130/60/50	1	1	281.81 ± 5.50	41.8 ± 0.8	3.8
Na29	M4c	30.3792	81.1845	4431	140/130/110	2	1	234.86 ± 4.12	35.2 ± 0.6	3.1
Na30	M4b	30.3773	81.1825	4398	140/120/60	2	1	284.47 ± 4.90	43.4 ± 0.8	3.9
Na31	M4b	30.3775	81.1821	4387	330/260/160	2	0.9664	290.74 ± 4.11	46.1 ± 0.7	4.1
Na32	M4b	30.3774	81.1819	4385	240/210/140	2	1	257.47 ± 5.58	39.5 ± 0.9	3.6
Na33	M4b	30.3775	81.1819	4378	320/200/140	2	1	290.43 ± 5.09	44.7 ± 0.8	4.0
Na34	M4b	30.3775	81.1815	4383	200/150/100	1	1	253.38 ± 6.14	38.6 ± 0.9	3.5
Na10	M4a	30.3817	81.1759	4515	200/160/40	1.5	1	188.66 ± 4.82	27.0 ± 0.7	2.5
Na11	M4a	30.3817	81.1760	4504	190/130/60	2.5	1	186.46 ± 4.70	27.0 ± 0.7	2.5
Na12	M4a	30.3816	81.1760	4500	150/120/70	5	1	364.95 ± 8.60	54.5 ± 1.3	5.0
Na13	M4a	30.3815	81.1757	4504	135/80/40	1	1	117.55 ± 3.11	16.8 ± 0.4	1.5
Na14	M4a	30.3812	81.1755	4501	450/400/400	1	1	62.30 ± 1.37	8.9 ± 0.2	0.8
Na15	M4a	30.3813	81.1757	4505	110/70/50	3	1	346.24 ± 6.79	50.7 ± 1.0	4.6
Na35	M3	30.3799	81.1736	4452	190/150/70	1	1	316.52 ± 7.46	46.7 ± 1.1	4.3
Na36	M3	30.3794	81.1730	4456	140/90/50	3	1	185.16 ± 4.38	27.6 ± 0.7	2.5
Na37	M3	30.3791	81.1726	4460	350/300/170	2	0.9818	196.48 ± 4.88	29.5 ± 0.7	2.7
Na38	M3	30.3788	81.1723	4460	170/140/80	1	1	433.12 ± 8.89	63.9 ± 1.3	5.8
Na39	M3	30.3780	81.1715	4446	200/190/120	6	1	352.67 ± 8.42	54.5 ± 1.3	5.0
Na40	M3	30.3778	81.1713	4436	190/110/110	1	1	431.43 ± 8.76	64.4 ± 1.3	5.8
Na41	M2	30.3789	81.1703	4444	150/75/40	1.5	1	472.63 ± 6.83	70.7 ± 1.0	6.3
Na42	M2	30.3789	81.1695	4448	140/130/110	1	1	715.45 ± 15.11	107.3 ± 2.3	9.9
Na43	M2	30.3791	81.1694	4445	190/170/70	3	1	584.97 ± 8.94	89.0 ± 1.4	8.0
Na45	M2	30.3806	81.1698	4453	110/100/130	2	1	457.35 ± 9.13	68.3 ± 1.4	6.2
Na46	M2	30.3796	81.1699	4454	110/80/60	1.5	1	414.34 ± 8.76	61.5 ± 1.3	5.6
Na47	M2	30.3795	81.1697	4456	160/110/60	3	1	496.92 ± 9.84	74.9 ± 1.5	6.8
Na18	M1c	30.3801	81.1657	4442	500/450/150	2	1	2082.40 ± 24.07	334.4 ± 4.2	31.9
Na19A	M1c	30.3809	81.1664	4445	550/480/170	1.5	1	2354.63 ± 24.77	380.4 ± 4.4	36.7
Na19B	M1c	30.3809	81.1664	4445	550/480/70	2	1	1975.17 ± 18.26	315.2 ± 3.2	29.9
Na20	M1c	30.3813	81.1677	4453	200/150/70	3	1	745.84 ± 9.56	113.7 ± 1.5	10.3
Na21	M1c	30.3832	81.1667	4455	320/250/130	1	1	2935.25 ± 24.71	481.6 ± 4.6	47.6
Na22	M1c	30.3832	81.1666	4459	380/180/160	1	1	2680.08 ± 22.31	433.8 ± 4.0	42.4
Na23A	M1c	30.3814	81.1681	4461	340/270/130	2	1	2183.51 ± 19.16	348.8 ± 3.3	33.3
Na23B	M1c	30.3814	81.1681	4461	340/270/0	1.5	0.9199	1656.79 ± 16.62	281.5 ± 3.0	26.5
Na1	M1b	30.3736	81.1591	4385	470/310/130	2	1	2642.20 ± 42.59	448.6 ± 8.1	44.5
Na2	M1b	30.3743	81.1593	4388	300/200/140	2	1	1931.93 ± 31.21	317.1 ± 5.6	30.4
Na3A	M1b	30.3753	81.1595	4401	240/220/150	1	1	1477.31 ± 16.59	234 ± 2.8	21.8
Na3B	M1b	30.3753	81.1595	4401	240/220/150	1.5	1	1430.04 ± 14.40	227.1 ± 2.4	21.1
Na4	M1b	30.3786	81.1598	4435	500/230/120	1	1	2577.80 ± 27.61	420.8 ± 5.0	41.1
Na5	M1b	30.3792	81.1603	4439	?	2	1	1081.99 ± 16.46	166.9 ± 2.7	15.4
Na6	M1b	30.3784	81.1592	4427	280/220/100	1.5	1	1763.49 ± 18.23	280.2 ± 3.1	26.3
Na7	M1b	30.3760	81.1583	4404	600/500/170	2	1	2712.17 ± 23.36	457.2 ± 4.4	44.9
Na8	M1b	30.3779	81.1567	4413	200/170/90	1.75	1	803.63 ± 9.26	123.9 ± 1.5	11.2
Na82	M1a	30.3957	81.1477	4373	200/95/85	1.5	1	501.63 ± 11.99	77.7 ± 1.9	7.1
Na83	M1a	30.3963	81.1466	4379	240/120/55	1	1	805.71 ± 10.91	125.5 ± 1.8	11.4
Na84	M1a	30.4000	81.1479	4395	190/170/80	2	1	1210.87 ± 17.22	191.9 ± 2.9	17.7
Na85	M1a	30.4008	81.1485	4394	270/200/70	2	1	1035.89 ± 14.40	163.0 ± 2.4	15.0
Na86	M1a	30.4003	81.1493	4402	550/400/190	2	1	1942.33 ± 15.47	316.3 ± 2.7	29.9
Na87	M1a	30.4009	81.1496	4403	600/400/140	2	1	1388.12 ± 17.60	220.7 ± 3.0	20.5
Muguru valley										
Na48	M10	30.4633	81.2169	5508	170/65/50	2	0.9464	2.90 ± 0.41	0.28 ± 0.04	0.05
Na49	M10	30.4634	81.2168	5506	130/120/30	1	0.9464	22.99 ± 0.65	2.2 ± 0.1	0.2
Na50	M10	30.4634	81.2169	5509	170/80/60	1.5	0.9464	0.75 ± 0.27	0.07 ± 0.03	0.03
Na52	M10	30.4640	81.2170	5514	140/100/25	1.5	0.9519	28.09 ± 0.69	2.7 ± 0.07	0.2
Na53	M10	30.4638	81.2159	5509	240/180/70	2	0.9554	1.78 ± 0.12	0.17 ± 0.01	0.02
Na54	M9	30.4637	81.2157	5503	120/100/60	1	0.9474	2.98 ± 0.39	0.28 ± 0.04	0.05
Na55	M9	30.4635	81.2157	5520	160/90/75	1.5	0.9474	3.09 ± 0.55	0.29 ± 0.05	0.1
Na56	M9	30.4629	81.2157	5509	220/150/70	2	0.9282	4.09 ± 0.36	0.40 ± 0.04	0.1
Na57	M9	30.4632	81.2155	5508	150/100/50	1	0.9331	6.69 ± 0.86	0.65 ± 0.08	0.1
Na58	M8	30.4683	81.2064	5325	110/90/50	5	1	38.41 ± 1.64	3.9 ± 0.17	0.4
Na59	M8	30.4683	81.2050	5325	180/160/80	1	1	29.51 ± 0.83	2.9 ± 0.1	0.3
Na64	M7	30.4704	81.2058	5195	100/100/40	2	0.98	26.5 ± 0.66	2.8 ± 0.1	0.3
Na66	M7	30.4711	81.2056	5159	210/120/100	5	0.9777	82.78 ± 2.37	9.2 ± 0.3	0.8
Na67	M7	30.4712	81.2056	5154	130/120/50	2	0.9777	57.37 ± 2.22	6.2 ± 0.2	0.6
Na68	M7	30.4712	81.2056	5154	130/70/40	1	0.9777	62.51 ± 1.84	6.7 ± 0.2	0.6
Na70	M6	30.4726	81.2044	5089	100/90/50	2	1	106.00 ± 2.73	11.6 ± 0.3	1.1
Na71	M6	30.4725	81.2044	5096	120/100/80	2.5	0.9777	3.41 ± 0.79	0.38 ± 0.09	0.1
Na75	M4	30.4744	81.1944	4842	150/125/60	3	1	431.87 ± 5.72	53.9 ± 0.7	4.8

Table 2 (*continued*)

Sample number	Landform	Latitude (°N)	Longitude (°E)	Altitude (m asl)	Boulder size a/b/c axis (cm)	Sample thickness (cm)	Shielding correction	^{10}Be atoms 10^4 per g of SiO_2	Age[a] (ka)	External error[b] (ka)
Na76	M4	30.4745	81.1943	4838	620/600/180	1	1	441.56 ± 10.41	54.3 ± 1.3	5.0
Na78	M4	30.4744	81.1940	4838	150/150/120	2	1	343.66 ± 5.28	42.5 ± 0.7	3.8
Na79	M4	30.4745	81.1933	4821	150/110/45	1	0.9774	288.70 ± 5.87	36.4 ± 0.7	3.3
Na80	M4	30.4751	81.1924	4786	190/110/90	1	1	355.01 ± 5.83	44.6 ± 0.7	4.0
Na81	M4	30.4758	81.1921	4766	120/70/45	2	1	3.98 ± 0.33	0.5 ± 0.04	0.1
Manarodi Valley										
Na113	M6	30.4298	81.4180	5531	400/200/300	2	1	143.90 ± 3.21	13.1 ± 0.3	1.2
Na114	M6	30.4302	81.4178	5533	160/100/40	2	1	136.15 ± 3.27	12.4 ± 0.3	1.1
Na116	M6	30.4316	81.4168	5540	220/110/90	3	1	222.54 ± 4.53	20.3 ± 0.4	1.8
Na104	M5	30.4365	81.4479	5499	230/200/40	2	1	132.16 ± 3.34	12.2 ± 0.3	1.1
Na105	M5	30.4364	81.4475	5501	220/140/70	1	1	79.56 ± 2.02	7.2 ± 0.2	0.7
Na106	M5	30.4363	81.4484	5499	200/170/80	2.5	1	137.55 ± 3.55	12.7 ± 0.3	1.2
Na107	M5	30.4365	81.4488	5500	340/180/60	2	1	165.76 ± 4.02	15.3 ± 0.4	1.4
Na108	M5	30.4373	81.4464	5497	220/180/40	1	0.9893	125.31 ± 3.15	11.6 ± 0.3	1.0
Na111	bedrock	30.4380	81.4464	5511	n/a	2	0.9884	119.29 ± 2.01	11.0 ± 0.2	1.0
Na112	bedrock	30.4379	81.4464	5515	n/a	2	0.9884	132.80 ± 2.34	12.3 ± 0.2	1.1
Na88	M4b	30.5397	81.4231	4802	210/130/80	2	1	120.12 ± 2.67	15.0 ± 0.3	1.4
Na89	M4b	30.5387	81.4238	4815	220/140/130	2.5	1	120.91 ± 2.13	15.1 ± 0.3	1.3
Na96	M4a	30.5422	81.4280	4762	160/100/70	3	1	390.86 ± 7.52	50.6 ± 1.0	4.6
Na97	M4a	30.5421	81.4280	4764	220/120/40	2	1	418.43 ± 10.10	53.7 ± 1.3	4.9

[a] The error is the internal uncertainty, which only takes into account the measurement uncertainty.
[b] The external uncertainty includes all uncertainties including the production rate uncertainty.

a specific time during the Lateglacial. M7 in the Muguru valley has ages that cluster around 6.3 ka and we suggest that this moraine formed during the Early Holocene. M8 through M10 in the Muguru valley have Neoglacial ages. ^{10}Be ages on M8 show that it likely formed several thousand years ago. The TCN ages on M9 and M10 show that they likely formed sometime between 0.1 ka and 2.7 ka. Given the position of M10 right next to the active glacier and that its ages are younger that M9, we argue that this moraine represents a Little Ice Age advance, with its older TCN ages reflecting some inheritance of TCNs due to prior exposure. Clearly any slight

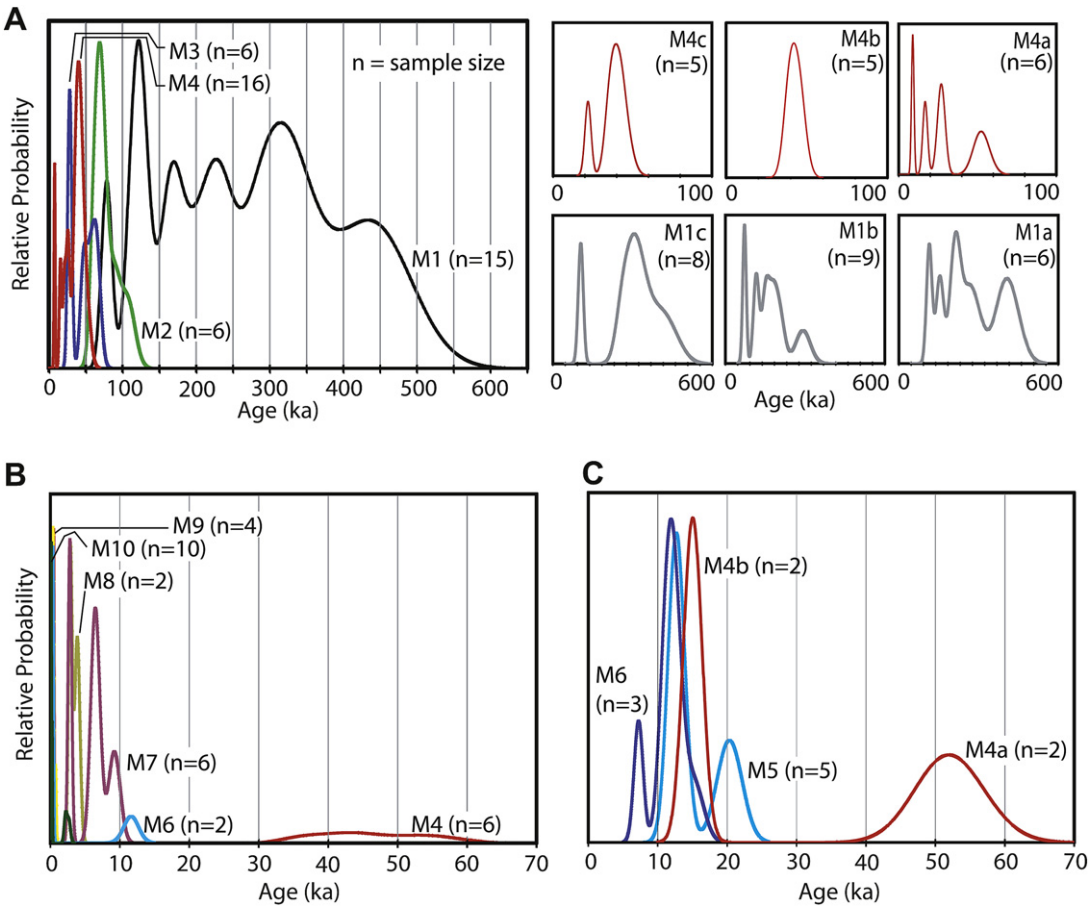

Fig. 10. Stacked probability distributions for ^{10}Be TCN surface exposure ages for each moraine in (A) the Ronggua valley foreland; (B) the Muguru valley; and (C) the Namarodi valley. The smaller graphs in part (A) are for each of the individual moraines dated for M1 and M4. The probability plots are constructed using the age and external error for each sample. Each plot has a relative scale based on the data examined therein.

Table 3
Moraine numbers, glaciations and ^{10}Be data for each study area (MIS = marine oxygen isotope stage).

Moraine name	Glaciation name after Ma (1989)	Sample size	Average age[a] (ka)	Maximum age (ka)	Range of ages (ka)	Assigned age (ka)
Ronggua Gorge foreland						
M4c	Namorangre	6	37 ± 8	46	22–46	MIS 3
M4b	Namorangre	5	43 ± 3	46	38–46	MIS 3
M4a	Namorangre	6	35 ± 17	51	9–55 ka	MIS 3
All M4	Namorangre	17	40 ± 9	51	9–55 ka	MIS 3
M3	Namorangre	6	48 ± 16	64	28–64	MIS-4/Early Last Glacial
M2	Rigongpu	6	79 ± 17	107	62–107	Early Last Glacial or MIS 6
M1c	Naimona'nyi	8	336 ± 111	482	114–482	MIS 10 or older
M1b	Naimona'nyi	9	297 ± 123	457	124–457	MIS 10 or older
M1a	Naimona'nyi	6	204 ± 83	316	78–316	MIS 10 or older
All M1	Naimona'nyi	23	281 ± 116	482	78–482	MIS 10 or older
Muguru valley						
M10	Neoglaciation	5	1.1 ± 1.3	2.7	0.1–2.7	Little Ice Age
M9	Neoglaciation	4	0.4 ± 0.2	0.7	0.3–0.7	Neoglacial
M8	Neoglaciation	2	3.4 ± 0.7	3.9	2.9–3.9	Neoglacial
M7	Neoglaciation	4	6.3 ± 2.6	9.2	2.8–9.2	Early Holocene
M6?	Neoglaciation	2	No average[b]	11.2	n/a	Lateglacial/Early Holocene
M4	Namorangre	6	46 ± 8	54	36–54	MIS 3
Namarodi valley						
M6	Neoglaciation	3	15.3 ± 4.4	20.3	12.4–20.3	Lateglacial
M5	Neoglaciation	5	12.9 ± 1.6	15.3	7.2–15.3	Lateglacial
M5 (bedrock)	Neoglaciation	2	11.7 ± 0.9	12.3	11.1–12.3	Lateglacial
M4b	Namorangre	2	15.0	15.1	15.0–15.1	MIS 3
M4a	Namorangre	2	52±2.2	54	51–54	MIS 3
All M4	Namorangre		n/a			

[a] Error expressed as 1σ.
[b] Because the difference between the two ages is so considerable (~12 ka cf 0.4 ka) an average age was not deemed realistic.

inheritance of ^{10}Be TCNs would greatly influence the young boulder's ages. In addition, the age may be affected by toppling and/or exhumation as the moraine stabilizes after glacial retreat, which will result in younger ages than the true age of the moraine (cf. Dortch et al., 2010).

6. Discussion

Glacial geologic evidence shows that glaciation on the Gurla Mandhata massif changes from expanded ice caps to deeply entrenched valley glaciers over the latter part of the Quaternary (Figs. 1–3). Assigning ages to the moraines produced during each glacial advance is challenging because of the problems associated with the application of TCN surface exposure dating methods. Nevertheless, we can broadly assign ages to the glacial succession on the Gurla Mandhata massif as discussed in the previous section. This shows that the oldest glaciation, Ma's (1989) Naimona'nyi glaciation, produced moraines considerably older than 300 ka and thus likely formed during MIS 10 or during an earlier glacial cycle. The moraines of the Naimona'nyi glaciation are among the oldest glacial landforms dated in the Himalayan–Tibetan orogen. Moraines of similar age are present in the Indus Valley in Ladakh where extensive valley glaciers advanced to an elevation below 3250 m asl at >430 ka (Owen et al., 2006a). Old glacier successions are also present in Muztag Ata and Kongur Shan where Seong et al. (2009) dated an expanded ice cap that advanced into the massif's foreland prior to the penultimate glacial cycle, in the Tanggula Shan where Schäfer et al. (2001) and Owen et al. (2005) dated moraines formed by an expanded ice cap to penultimate glacial cycle, and in the Rongbuk valley, north of Mt Everest, where Owen et al. (2009) dated erratics to >330 ka, which represented extensive valley glaciers. In addition, Owen et al. (2006b), Chevalier et al. (2005) and Schäfer et al. (2008) dated moraines that they argued formed during the penultimate or an earlier glacial cycle in the Ayalari Range, Nyalam and Kunlun Shan, respectively.

Our ^{10}Be dating shows that another glaciation (M2), the Rigongpu glaciation of Ma (1989), with moraines ranging in age from 62 to 107 ka, occurred during the early part of the last glacial cycle or if the younger ^{10}Be ages in the distribution are the result of weathering and/or exhumation then this would formed during the penultimate glacial cycle. During this glaciation the piedmont glaciers extended a few kilometers beyond the mountain front and coalesced with each other. The large time lag between the Naimona'yni and Rigongpu glaciation (300 ka cf. ~62–107 ka) is intriguing. It suggests that either there was no significant advance during this time interval, or that we did not recognize evidence for a glaciation in this interval because glaciers did not advance beyond the Riogongpu glacier limits and their evidence was destroyed by the later, more extensive Rigongpu glaciation.

The Rigongpu glaciation of Ma (1989) was followed by a change in glacial style to entrenched valley glaciers. The oldest two of these glacial advances (M3 and M4) occurred during the Namorangre glaciation of Ma (1989) when glaciers advanced to the mouths of most valleys throughout the massif (Fig. 3). Boulders from M3 glaciers range in age between 28 and 64 ka and two sets of M2 glacial boulders yield mean ages of 40 ± 9 and 52 ± 2 ka, dating to the early part of the last glacial cycle and MIS 3. Numerous studies have shown that glaciers advanced during MIS 3 throughout the Himalaya and Tibet, and that these advances were more extensive than those associated with MIS 2 (e.g. Finkel et al., 2003; Owen et al., 2002, 2003a, 2005, 2006b, 2009; Seong et al., 2009).

A succession of at least six sets of moraines is present within the valleys to the contemporary glaciers, which Ma (1989) attributes to the Neoglacial. Our ^{10}Be dating of these moraines shows that they represent a much longer duration of glacier oscillations extending from the Lateglacial to the Little Ice Age. ^{10}Be ages on the M5 and M6 in the Namarodi valley suggest that they formed sometime during the Lateglacial. Similar Lateglacial advances have been recognized elsewhere in the Himalaya (Finkel et al., 2003; Owen et al., 2001, 2002, 2003a,b,c, 2005), but assigning any ^{10}Be dated moraine to a specific time during the Lateglacial is challenging because the associated uncertainty with the age is quite large (usually >10%). It is likely that some of the moraines represent advances during the Lateglacial Interstadial and/or Early Holocene,

representing times of increased moisture supply and thus positive glacier mass balances.

Moraine M7 in the Muguru valley has ^{10}Be ages that cluster around 6.3 ka, which suggests that this moraine formed during the Early Holocene. Glaciation during the Early Holocene is very pervasive throughout the Himalaya and Tibet and likely represents positive glacier mass balances related to enhanced moisture supply and increased cloudiness to the Himalaya during a time of increased insolation (Finkel et al., 2003; Owen et al., 2001, 2002, 2003a,b,c, 2005, 2006a,b, 2009; Seong et al., 2009; Zech et al., 2003; Rupper et al., 2009).

Moraines M8 through M10 in the Muguru valley have Neoglacial ages. M8 likely formed several thousand years ago, while ^{10}Be ages on M9 and M10 show that they possibly formed ~1000 years ago. M10, however, might have formed during the Little Ice Age. Owen (2009) discusses the nature of Neoglacial glacier fluctuations in the Himalaya and Tibet and highlights the abundance of evidence for significant Neoglacial advances in most regions, but also emphasizes the uncertainty in defining the age of the Little Ice Age in the Himalaya and Tibet, and also in assigning moraines to the Little Ice Age. Seong et al. (2009) showed that throughout the Lateglacial and Holocene, glaciers in Muztag Ata and Kongur Shan have likely been responding to Northern Hemisphere climate oscillations (rapid climate changes), with minor influences from the south Asian monsoon. This might be the case for Gurla Mandhata, but more numerical dating of the moraine successions is needed to test this possibility.

Explaining the change of style of glaciation from expanded ice caps to entrenched valley glacier systems on Gurla Mandhata is difficult. Similar changes in the style of glaciation have been recognized elsewhere in the Himalayan–Tibetan orogen, including Tanggula Shan, and Muztag Ata and Kongur Shan (Owen et al., 2005; Seong et al., 2009). Owen et al. (2005) argued that the regional patterns and timing of glaciation throughout the Himalayan–Tibetan orogen likely reflect temporal and spatial variability in the south Asian monsoon and, in particular, regional precipitation gradients. Owen et al. (2005) believed that in zones of greater aridity, the extent of glaciation has become increasingly restricted throughout the Late Quaternary leading to the preservation of old glacial landforms (100 ka), whereas in regions that are very strongly influenced by the monsoon ($\leq$1600 mm a^{-1}), the preservation potential of pre-Lateglacial moraine successions is generally extremely poor. This is possibly because Lateglacial and Holocene glacial advances may have been more extensive than earlier glaciations and hence may have destroyed any landform or sedimentary evidence for the earlier glaciations. Furthermore, Owen et al. (2005) argued that the intense denudation, which characterizes these wetter environments results in rapid erosion and re-sedimentation of glacial and associated landforms, which also contributes to their poor preservation potential.

Seong et al. (2009) suggested that the change in style of glaciation in Muztag Ata and Kongur Shan likely represents a significant reduction over the last few glacial cycles of the moisture flux to the region that is needed to maintain positive glacier mass balances. Similarly this could be the case in Gurla Mandhata. Furthermore, Seong et al. (2009) went on to hypothesize that this might reflect a change in regional climatic forcing that might be the result of the progressive surface uplift of the adjacent mountain ranges that restricted the supply of moisture by the monsoon and westerlies to the region. Although we cannot test this at present similar factors might have controlled the style of glaciation in Gurla Mandhata. Similar arguments regarding uplift of mountains and reduced moisture supply were proposed by Owen et al. (2006a) for progressive restriction of glaciation in Ladakh over the last 400 ka. However, drawing links between mountain uplift and changes in regional climate is very tentative because it is not possible to define the timing and magnitude of surface uplift for most mountain ranges. In addition, the similar pattern of progressive restriction of glaciation over the last ~400 ka for the Transhimalaya (Owen et al., 2005, 2006a, 2008) and the more arid areas of Tibet suggests that regional climate change rather than localized tectonics is responsible for the pattern of glaciation. Furthermore, Owen et al. (2006a) and Seong et al. (2009) pointed out that in other mountain regions of the world, such as Tasmania, the Sierra Nevada, Alaska, the Peruvian Andes, Patagonia, and the Chilean Lake District, glaciation has also become progressively less extensive over time. This suggests that the decreasing extent of mountain glaciation globally, and specifically for Gurla Mandhata based on the chronology presented here, over at least the last 400 ka may be related to a global pattern of climate change. The reason for this changing pattern of glaciation, however, has yet to be resolved.

Muztag Ata and Kongur Shan, and Gurla Mandhata, however, add an extra complexity to the argument for forcing due to climate change. Both areas are experiencing active detachment faulting that is resulting in the rapid exhumation of bedrock and adjacent basin formation (Arnaud et al., 1993; Murphy et al., 2000, 2002). The pattern of glaciation in these two regions, although separated by >1000 km at either end of the Karakoram Fault, is remarkably similar in style. The rapid exhumation in both regions might be broadly equated to the growth of the two massifs, which initiated glaciation as ice caps when the massifs became sufficiently high to enhance orographic precipitation. As the adjacent basins deepened, during times of deglaciation, rivers rapidly incised deep valleys into Gurla Mandhata, which were then occupied by glaciers during later glacial times, resulting in entrenchment of the glaciers. Although the change in vertical relief is not well defined, it could be as much as 500 m in the last 1 Ma based from the amount of extension determined by Murphy et al. (2000, 2002). Whether this is enough to cause a change in the pattern of glaciation is not known. This tectonic explanation for changing the style of glaciation does not really explain the decrease in total ice volume over time. The pattern of glaciation we see in both the Muztag Ata and Kongur Shan, and Gurla Mandhata regions, however, might reflect a combination of these regional climatic and tectonic geomorphic controls.

These intriguing changes in patterns of glaciation clearly need to be examined more widely throughout the Himalaya and Tibet, and our study leaves many questions open for debate, such as how important is local and regional tectonics, and/or topography are in controlling glacial style, timing and extent. Our data, however, provide the first comprehensive chronostratigraphy for the Gurla Mandhata massif, which in turn should help form a structure to understand the nature of glaciation in southern Tibet and the northernmost Himalaya. In addition, the glacial chronology that is provided forms a framework for future studies that may examine the relationships among climate, glaciation, erosion, and landscape development in the Himalayan–Tibetan orogen.

7. Conclusions

Ten sets of moraines have been dated using ^{10}Be TCNs on the Gurla Mandhata massif. The oldest moraines, produced during the Naimona'nyi glaciation of Ma (1989), likely formed during MIS 10 or an earlier glacial cycle by an expanded ice cap that stretched ~5 km into the foreland of the massif. This was followed by a glacial expansion resulting in piedmont glaciers extending a few kilometers beyond the mountain front. This glacial expansion is the Rigongpu glaciation of Ma (1989) and occurred during the early part of the last glacial cycle or the penultimate glacial cycle. This glaciation was followed by a change in glacial style to entrenched valley glaciers that produced impressive latero-frontal moraines.

The oldest of these glacial advances in the Rigongpu glaciation produced moraines that occur at the mouths of most valleys and date to MIS 6 or the early part of the last glacial cycle. This glacial advance was followed by a later glacial advance, which is dated to early last glacial or MIS 4, and followed by an advance that is dated to MIS 3. These two glacial advances occurred during the Namorangre glaciation of Ma (1989). A succession of six sets of moraines within the valleys of Gurla Mandhata up to the contemporary glaciers represent glacial advances that occurred during the Late-glacial, Early Holocene, Neoglaciation and possibly Little Ice Age.

Glaciation on the Gurla Mandhata massif changed from expanded ice caps to deeply entrenched valley glaciers between at least the time of MIS 10 to the beginning of the last glacial. Explaining this change in the style of glaciation is difficult, but it might be due to changes in regional climate, which by comparison with other Tibetan and Transhimalayan regions suggests that glaciation became very restricted in extent over the Middle and Late Pleistocene. Alternatively, the change in style of glaciation might reflect tectonic controls such as increasing basin subsidence due to active detachment faulting and enhanced valley incision associated with increased relative relief and greater slopes to produce entrenched glaciation. It is likely, however, that a combination of climatic and tectonic controls is responsible for the change in style of glaciation.

Our dating provides the first quantitative chronology for the Gurla Mandhata massif and forms a structure to help understand the nature of glaciation, climate change, erosion and landscape development in southern Tibet and northernmost Himalaya.

Acknowledgements

Part of this work was undertaken at the Lawrence Livermore National Laboratory (under DOE Contract W-7405-ENG-48). Chaolu Yi was supported in part by CAS grant (kzcx2-yw-104) and NSFC grant (40730101 and 40671023). We are grateful to Jason Dortch, Kate Hedrick and Craig Dietsch for comments on this manuscript. Special thanks to Yeong Bae Seong and Jakob Hyman for their very constructive and detailed reviews of our paper.

References

Arnaud, N.O., Brunel, M., Cantagrel, J.M., Tapponnier, P., 1993. High cooling and denudation rates at Kongur Shan, eastern Pamir (Xinjiang, China) revealed by $^{40}Ar/^{39}Ar$ alkali feldspar thermochronology. Tectonics 12, 1335–1346.

Balco, G., Briner, J., Finkel, R.C., Rayburn, J., Ridge, J.C., Schaefer, J.M., 2008a. Regionalberyllium-10 production rate calibration for late-glacial northeastern North America. Quaternary Science Reviews 4, 93–107.

Balco, G., Stone, J.O., Lifton, N.A., Dunai, T.J., 2008b. A complete and easily accessible means of calculating surface exposure ages or erosion rates from ^{10}Be and ^{26}Al measurements. Quaternary Geochronology 8, 174–195.

Benn, D.I., Owen, L.A., 2002. Himalayan glacial sedimentary environments: a framework for reconstructing and dating former glacial extents in high mountain regions. Quaternary International 97/98, 3–26.

Briner, J.P., Kaufman, D.S., Manley, W.F., Finkel, R.C., Caffee, M.W., 2005. Cosmogenic exposure dating of late Pleistocene moraine stabilization in Alaska. Geologic Society of America Bulletin 117, 1108–1120.

Chevalier, M.-L., Ryerson, F.J., Tapponnier, P., Finkel, R.C., Van Der Woerd, J., Haibing, L., Qing, L., 2005. Slip-rate measurements on the Karakoram Fault may imply secular variations in fault motion. Science 307, 411–414.

Dortch, J., Owen, L.A., Caffee, M.C., Brease, P., 2010. Late Quaternary glaciation and equilibrium line altitude variations of the McKinley River region, central Alaska Range. Boreas 39, 233–246.

Finkel, R.C., Owen, L.A., Barnard, P.L., Caffee, M.W., 2003. Beryllium-10 dating of Mount Everest moraines indicates a strong monsoonal influence and glacial synchroneity throughout the Himalaya. Geology 31, 561–564.

Hallet, B., Putkonen, J., 1994. Surface dating of dynamic landforms: young boulders on aging moraines. Science 265, 937–940.

Lal, D., 1991. Cosmic ray labeling of erosion surfaces: in situ nuclide production rates and erosion models. Earth and Planetary Science Letters 104, 429–439.

Ma, Q.H., 1989. Geomorphology and Quaternary glaciations in Naimona'nyi Peak region. In: Shidei, T. (Ed.), Proceedings of the Sino-Japanese Joint Scientific Symposium Tibetan Plateau, vol. 2, pp. 41–54. 218–231.

Miehe, G., Winiger, M., Bohner, J., Yili, Z., 2004. Climatic Diagram Map of High Asia, 1:4,000,000.

Murphy, M.A., Yin, A., Kapp, P., Harrison, T.M., Durr, S.B., Ding, L., Guo, J., 2000. Southward propagation of the Karakoram fault system, southwest Tibet: timing and magnitude of slip. Geology 25, 719–722.

Murphy, M.A., Yin, A., Kapp, P., Harrison, T.M., Manning, C.E., Ryerson, F.J., Ding, L., Guo, J., 2002. Structural evolution of the Gurla Mandhata detachment system, southwest Tibet: implications for the eastward extent of the Karakoram fault system. Geological Society of America Bulletin 114, 428–447.

Nishiizumi, K., Imamura, M., Caffee, M.W., Southon, J.R., Finkel, R.C., McAninch, J., 2007. Absolute calibration of ^{10}Be AMS standards. Nuclear Instruments & Methods in Physics Research–Beam Interactions with Materials and Atoms 258B, 403–413.

Owen, L.A., 2009. Latest Pleistocene and Holocene glacier fluctuations in the Himalaya and Tibet. Quaternary Science Reviews 28, 2150–2164.

Owen, L.A., Gualtieri, L., Finkel, R.C., Caffee, M.W., Benn, D.I., Sharma, M.C., 2001. Cosmogenic radionuclide dating of glacial landforms in the Lahul Himalaya, northern India: defining the timing of Late Quaternary glaciation. Journal of Quaternary Science 16, 555–563.

Owen, L.A., Finkel, R.C., Caffee, M.W., Gualtieri, L., 2002. Timing of multiple Late Quaternary glaciations in the Hunza Valley, Karakoram Mountains, northern Pakistan: defined by cosmogenic radionuclide dating of moraines. Geological Society of America Bulletin 114, 593–604.

Owen, L.A., Finkel, R.C., Ma, H., Spencer, J.Q., Derbyshire, E., Barnard, P.L., Caffee, M. W., 2003a. Timing and style of Late Quaternary glaciations in NE Tibet. Geological Society of America Bulletin 115, 1356–1364.

Owen, L.A., Ma, H., Derbyshire, E., Spencer, J.Q., Barnard, P.L., Zeng, Y.N., Finkel, R.C., Caffee, M.W., 2003b. The timing and style of Late Quaternary glaciation in the La Ji Mountains, NE Tibet: evidence for restricted glaciation during the latter part of the Last Glacial. Zeitschrift für Geomorphologie 130, 263–276.

Owen, L.A., Spencer, J.Q., Ma, H., Barnard, P.L., Derbyshire, E., Finkel, R.C., Caffee, M. W., Zeng, Y.N., 2003c. Timing of Late Quaternary glaciation along the southwestern slopes of the Qilian Shan, Tibet. Boreas 32, 281–291.

Owen, L.A., Finkel, R.C., Barnard, P.L., Haizhou, M., Asahi, K., Caffee, M.W., Derbyshire, E., 2005. Climatic and topographic controls on the style and timing of Late Quaternary glaciation throughout Tibet and the Himalaya defined by ^{10}Be cosmogenic radionuclide surface exposure dating. Quaternary Science Reviews 24, 1391–1411.

Owen, L.A., Caffee, M.W., Bovard, K.R., Finkel, R.C., Sharma, M.C., 2006a. Terrestrial cosmogenic nuclide surface exposure dating of the oldest glacial successions in the Himalayan orogen. Ladakh Range, northern India. Geological Society of America Bulletin 118, 383–392.

Owen, L.A., Finkel, R.C., Ma, H., Barnard, P.L., 2006b. Late Quaternary landscape evolution in the Kunlun Mountains and Qaidam Basin, Northern Tibet: a framework for examining the links between glaciation, lake level changes and alluvial fan formation. Quaternary International 154/155, 73–86.

Owen, L.A., Caffee, M.W., Finkel, R.C., Seong, B.Y., 2008. Quaternary glaciations of the Himalayan–Tibetan orogen. Journal of Quaternary Science 23, 513–532.

Owen, L.A., Robinson, R., Benn, D.I., Finkel, R.C., Davis, N.K., Yi, C., Putkonen, J., Li, D., Murray, A.S., 2009. Quaternary glaciation of Mount Everest. Quaternary Science Reviews 28, 1412–1433.

Putkonen, J., Swanson, T., 2003. Accuracy of cosmogenic ages for moraines. Quaternary Research 59, 255–261.

Putkonen, J., O'Neal, M.A., 2006. Degradation of unconsolidated Quaternary landforms in the western North America. Geomorphology 75, 408–419.

Putkonen, J., Connolly, J., Orloff, T., 2008. Landscape evolution degrades the geologic signature of past glaciations. Geomorphology 97, 208–217.

Rupper, R., Roe, G., Gillespie, A., 2009. Spatial patterns of Holocene glacier advance and retreat in Central Asia. Quaternary Research 72, 337–346.

Schäfer, J.M., Tschudi, S., Zhao, Z., Wu, X., Ivy-Ochs, S., Wieler, R., Baur, H., Kubik, P. W., Schluchter, 2001. The limited influence of glaciations in Tibet on global climate over the past 170000 yr. Earth and Planetary Science Letters 6069, 1–11.

Schäfer, J.M., Oberholzer, P., Zhao, Z., Ivy-Ochs, S., Wieler, R., Baur, H., Kubik, P.W., Schlüchter, C., 2008. Cosmogenic beryllium-10 and neon-21 dating of late Pleistocene glaciations in Nyalam, monsoonal Himalayas. Quaternary Science Reviews 27, 295–311.

Seong, Y.B., Owen, L.A., Bishop, M.P., Bush, A., Clendon, P., Copland, P., Finkel, R., Kamp, U., Shroder, J.F., 2007. Quaternary glacial history of the Central Karakoram. Quaternary Science Reviews 26, 3384–3405.

Seong, Y.B., Owen, L.A., Bishop, M.P., Bush, A., Clendon, P., Copland, P., Finkel, R., Kamp, U., Shroder, J.F., 2008. Reply to comments by Matthias Kuhle on "Quaternary glacial history of the central Karakoram". Quaternary Science Reviews 27, 1656–1658.

Seong, Y.B., Owen, L.A., Yi, C., Finkel, R.C., 2009. Quaternary glaciation of Muztag Ata and Kongur Shan: evidence for glacier response to rapid climate changes throughout the Late Glacial and Holocene in westernmost Tibet. Geological Society of America Bulletin 121, 348–365.

Stone, J.O., 2000. Air pressure and cosmogenic isotope production. Journal of Geophysical Research 105, 23753–23759.

Zech, W., Glaser, B., Abramowski, U., Dittman, C., Kubik, P.W., 2003. Reconstruction of the Late Quaternary Glaciation of the Macha Khola valley (Gorkha Himal, Nepal) usingrelative and absolute (^{14}C, ^{10}Be, dendrochronology) dating techniques. Quaternary Science Reviews 22, 2253–2265.